Pharmacophore 2014, Vol. 5 (6), 857-866 USA CODEN: PHARM7 ISSN 2229-5402

Pharmacophore

(An International Research Journal)

Available online at http://www.pharmacophorejournal.com/

Original Research Paper

2D AND 3D QSAR STUDIES OF INDOLIZINO [6, 7-B] INDOLE DERIVATIVES AS TOPOISOMERASE I AND II DUAL INHIBITORS

Anuj Kale[1], **Sachin Wakadkar[1]***, Madhuri Nagras[1] and Vijay Khedkar[2]

[1]Department of Pharmaceutical Chemistry, Sinhgad College of Pharmacy, STES Campus, Off Sinhagad Road, Pune-411 041, India

[2]National Chemical Laboratories, Pune, India

ABSTRACT

Topoisomerase is an essential enzyme required for DNA replication and hence playing a pivotal role in oncology. Known and validated target in anticancer drug discovery, and the well-established link between the higher enzyme activity and malignancy, makes topoisomerase an excellent target. In this study, a series of 36 topoisomerase I and II dual inhibitors, having indolizino[6,7-b]indole ring system as the core scaffold, was subjected to molecular modelling study. Molecular attributes such as steric, electrostatic and hydrogen bonding and their effect on biological activity were established using 3D QSAR tools; comparative molecular field analysis (CoMFA) and comparative molecular similarity indices analysis (CoMSIA). Dual inhibition and indole ring may make these molecules potential anticancer agents. Robust and statistically sound model was derived having significant r^2 and r^2_{pred} values giving better understanding of crucial regions around the scaffold to afford better activity. Dividing the series into test and training sets allowed calculations validating the predictive ability of the model. The contour maps and statistical analyses may provide positive assistance in developing similar molecules in future.

Keywords: Topoisomerase, HQSAR, CoMFA, CoMSIA, indolizino[6,7-b]indole, Cancer, Dual inhibition.

INTRODUCTION

Eukaryotic topoisomerase I (Topo I) is a crucial enzyme required for many significant cellular processes owing to its ability to relax the double-helix structure of DNA to allow access to the genetic information stored within during activities like DNA replication, transcription, and repair.[1] In a similar fashion, Topoisomerase II (Topo II) creates double-strand breaks and allows passage of double-stranded DNA via the incision to permit relaxation of over-coiled DNA.[2] Since topoisomerases are involved in various processes such as replication, recombination, chromosome segregation and transcription, these enzymes have the ability to solve topological challenges related to DNA double helical structure by cleaving and resealing DNA strands. Topo I and Topo II, through diverse mechanisms, play a very crucial role of DNA processing needed for the separation of chromosomes in order to complete mitosis.[3] Topoisomerase inhibitors have been widely used as anticancer agents. Topo I inhibitors, the camptothecin analogs irinotecan and topotecan have been reported for the treatment of colon cancer.[4] Presently two water-soluble derivatives of camptothecin, Irinotecan (CPT-11) for the treatment of colorectal tumors and Topotecan for the treatment of ovarian cancers and small-cell lung cancers (SCLC) approved by the FDA for IV administration.[5] Topo II inhibitors such as epirubicin, idarubicin, doxorubicin, daunorubicin,

teniposide, etoposide, and mitoxantrone are notable drugs used in the therapy of many malignancies including those of lungs, breast, testes and lymphomas and sarcomas.[6] Recently, it has been observed that dual inhibitors of topoisomerase I and II have shown significant cytotoxic effects and relatively low toxicity thus increasing the demand to study them further deeply.[7-9]

The purpose of this research is to understand and correlate the molecular bases and their corresponding biological activities with the help of computational chemical analyses.

MATERIALS AND METHODS

Computational Details

The study was performed using molecular modelling package Sybyl-X (v2.0, Tripos Inc., USA) running on Intel Core2(TM) Duo computer under the Windows OS was used in this modelling study.

Ligand Preparation

The set of 36 topoisomerase inhibitors was selected from literature.[10] The compounds taken for study are shown in the following figure. In present study, the negative log of IC_{50} (pIC_{50}) values were used, since it affords significantly larger numerical values for the active molecules than those for the inactive molecules. The obtained pIC_{50} values were used as the dependent variable in the 3D-QSAR study. The 3D-structures of the molecules were drawn using the *Builder* module of Sybyl. The structures were processed to attain the global minimum energy structures, which are thought to be the bioactive conformations. Energy minimization of the ligands was carried out using the Powel gradient method, the Tripos force field, Gasteiger Hückel charges and a distance dependent dielectric, till a gradient of 0.01 kcal mol−1 Å−1 was achieved. The set of molecules was divided into training set of 28 molecules and test set of 8 molecules. Molecules of the test set were chosen owing to their chemical diversities among the entire set and their varying potencies.

Comparative Molecular Field Analysis (CoMFA) and Comparative Molecular Similarity Indices Analysis (CoMSIA) and Hologram Quantitative Structure Activity Relationship (HQSAR) Studies

CoMFA has been exploited to calculate forces such as polar, hydrophobic, electrostatic, and steric interactions working between drugs and their biological targets determining their interactions. Quantitative Structure Activity Relationship (QSAR) tools like CoMFA obtain a mathematical pattern where the degree of biological activity is compared with the three dimensional properties of the compounds. Depending upon the patterns derived using such QSAR tools, biological activities of the untested molecules can be predicted and the structural changes required in the existing compounds can be predicted to afford novel molecules with better activities. A broad set of physicochemical descriptors such as structural, conformational, geometric, electronic, and thermodynamic properties are used to derive a pattern in CoMFA.[11] CoMSIA consists of aligning molecules under study based on either structure or field, followed by generating a rectangular grid enclosing the molecular mass evenly. A probe atom is placed in this hypothetical system to measure forces like electrostatic, steric, hydrophobic, H-bond donor or acceptor fields within the rectangular field. Then, the results from the field grid are combined with their reported biological activities from the compounds under study are put into a table and partial least squares (PLS) is applied to obtain the final CoMSIA model.[12-13] HQSAR is a relatively simpler technique of QSAR analysis in contrast to 3D analyses requiring no need to generate and align the molecules under study thus taking lesser time and computational prowess to derive the QSAR model. This analysis highlights contributions of every individual molecules towards their corresponding biological activities.

The relationship between 2D fingerprint and biological activity is determined using PLS methodology. HQSAR model was generated using structural features of descriptors as independent variables and pIC_{50} values as dependent variables. Statistical analyses are presented in table 4.

Statistical Analysis

The CoMFA and CoMSIA field energies were used as independent variables while the pIC_{50} values formed the dependent variables. A partial least squares (PLS)[14] regression was then run to obtain the 3D-QSAR models. Evaluation of the predictive ability of the obtained statistical models was performed using the "leave-one-out" (LOO) cross-validation procedure.[15-16] This method involves logical exclusion of each molecule from the data set and its activity predicted by a model which is then deduced from the residual molecules. To minimize the possibility of over fitting data, the number of components referring to the least PRESS value was used to obtain the ultimate PLS regression models. SAMPLS[17] method with leave-one-out (LOO) validation with no column filtering were used for cross-validation calculations to determine the q^2 (r^2_{cv}) and standard error of prediction (SEP). The PLS analysis was repeated without cross-validation with the optimum number of components and the conventional correlation coefficient r^2, the standard errors (SE) and the F-value were obtained. Comprehensive data is presented in table 4.

RESULTS

A number of 3D-QSAR models were derived and the best was chosen based on their statistical parameters. The statistical parameters for the 3D-QSAR models derived are given in Table

CoMFA Analysis

28 of the total 36 indolizino [6,7-b]indole derivatives formed the training set and the remaining 8 molecules constituted of the test set. These two sets of molecules were used to derive and validate the CoMFA model based on atom fit alignment. The training and test set molecules were selected such that their structural diversities and range of potency in the dataset was maintained. For the CoMFA model generated, partial least squares (PLS) regression produced a cross-validated correlation coefficient q^2 of 0.755 with 6 components. The non cross-validated PLS analysis produced a correlation coefficient (r^2) of 0.959, F value of 81.478 and an estimated standard error (SE) of 0.163. The steric field descriptors explain 91.3% of the variance, while the electrostatic descriptors explain 8.7% of the variance, signifying that the contribution of the steric field is dominant. The model was checked for its robustness the bootstrap analysis. The bootstrap analysis gave a correlation coefficient (r^2_{bs}) of 0.977 which supports the statistical validity of the derived CoMFA model. The possibility of chance correlation was eliminated by performing Y-scrambling. The correlation coefficient r^2 of 0.1 was obtained. Difference between the CoMFA model and y-scrambled model shows credibility of the former.

CoMSIA Analysis

The CoMSIA analysis was performed with the same structural alignment of molecules and same size of training and test sets as stated in the CoMFA studies. The analysis gave the fields holding importance which were steric, electrostatic and H-bond donor fields influencing molecules' potency. Combination of these fields yielded a q^2 value of 0.728 with 5 components, non cross validated r^2 of 0.908 having standard error of prediction of 0.243, F value as 34.692 with bootstrap r^2 value of 0.945. Y-scrambling yielded r^2 of 0.15 suggesting an extremely low probability of chance correlation. The steric, electrostatic and hydrogen bond acceptor contributions of the obtained model were 54.9, 35.6 and 9.5%, respectively. Hydrogen bond donor contribution was found to be significantly poor.

HQSAR Analysis

The test and training sets used were kept same as those used for CoMFA and CoMSIA. The best hologram model was generated using HL of 97 having two optimum components. Bonds, hydrogen atoms and donor–acceptor properties were used as descriptors. The best generated model gave cross-validated r2 (q2) of 0.881 and non-cross-validated r2 value of 0.900 with standard errors of 0.413 and 0.254 respectively. The total collection of these generated models comprises ensemble, and the ensemble value for r2 was calculated to be 0.894.

DISCUSSION

Predictivity of CoMFA, CoMSIA and HQSAR Models

The 3D-QSAR models were evaluated for their predictive powers by having the test set molecules excluded in the development of the models. External validation is thought to provide a validation for a predictive QSAR model, owing to complete exclusion of the test set molecules during the training of the model. The predicted pIC_{50} values were found to be in good accordance with the experimental outputs within a statistically tolerable error range. The predictive correlation coefficient r^2_{pred} for CoMFA and CoMSIA models derived was 0.713 and 0.768 respectively.

CoMFA Contour Maps

The steric interactions are represented by green and yellow regions, where increase in activity is associated with more bulk near the green and less bulk near the yellow contours. The scaffold chosen for the CoMFA contour map is indolizino[6,7-b]indole depicted in figure 1. As seen in the CoMFA contour map, bulky groups at R_3 and R_4 positions of the scaffold are required to afford activity whereas bulky groups near R_2 decrease the activity. This phenomenon can be observed peculiarly in the case of molecule **7** where bulky groups; ethyl isopropylcarbamate are present at R_3 and R_4 and least bulky methyl group is present at R_2. This molecule is the most potent in activity. Similarly, molecule **4** carrying a relatively lesser bulky ethyl ethylcarbamate groups at R_3 and R_4 with least bulky methyl group at R_2 is the second most potent molecule. Whereas, molecule **15** exhibiting bulky 2-chloro-1-fluoro-4-methylbenzene at R_2 and very little bulky ethanol groups at R_3 and R_4 make it the least potent molecule. Molecule **14** having bulky 1,2-difluoro-4-methylbenzene groups at R_3 and R_4 with ethanol at R_2 also shows little potency. Electrostatic CoMFA contour map reveals requirement of electronegative groups near R_3 and R_4 and very little electropositive element near R_2. One of the most active molecules; molecules **9** and **25** possess electronegative N and O among the substituent groups at R_3 and R_4 giving them sufficient electronegativity at the said positions where it is required the most to exhibit activity as per the derived contour map. Whereas low activity of molecules **13** and **15** can be attributed to lesser electronegative groups like –OH at R_3 and R_4 combined with highly electronegative halogens present in substituents at R_2 where such arrangement is disfavored.

CoMSIA Contour Maps

Similar to the CoMFA contour map outcome, CoMSIA contour map suggests requirement of bulky steric at positions R_3 and R_4 of the indolizino[6,7-b]indole scaffold depicted in figure 1 to afford good activity as observed in molecules **19** and **28**. Electrostatic contour map is also in agreement with CoMFA electrostatic contour map favouring electropositive groups at R_2 and electronegative groups at R_3 and R_4 to exhibit greater biological activities such as in cases of molecules **29** and **36** where former possessing a phenyl group shows significantly more potency than the latter containing a trimethoxy phenyl moiety.

CONCLUSION

The 3D QSAR models derived in this study corroborate molecular fundamentals for topoisomerase inhibition and eventual anticancer activity. The models derived here show good validity and consistency. The ability to predict via these models show a healthy correlation between experimentally determined and predicted pIC_{50} values considering the test set. Contour maps of CoMFA and CoMSIA analyses and HQSAR findings provide an important relationship between spatial arrangement and activities afforded. These models may be used as templates to design novel topoisomerase I and II inhibitors with having better potencies.

ACKNOWLEDGEMENTS

This work was carried out with the help of financial funding from BCUD, University of Pune We would like to thank Sinhgad Technical Education Society for providing us with required equipment.

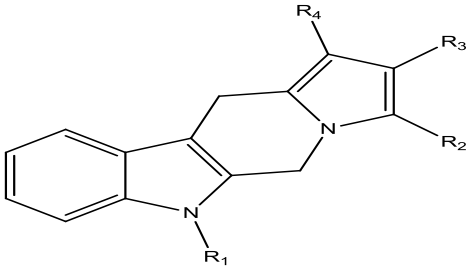

Figure 1: Indolizino[6,7-b]indole core scaffold

Table 1: Indolizino[6,7-b]indole Derivatives taken for 3D QSAR study

Mol. ID	R_1	R_2	R_3	R_4	IC_{50} (µM) (CCRF/CEM)
1	Me	Me	CH_2OH	CH_2OH	0.04
2	Et	Me	CH_2OH	CH_2OH	0.10
3	Bn	Me	CH_2OH	CH_2OH	0.29
4	Me	Me	$CH_2OCONHEt$	$CH_2OCONHEt$	0.04
5	Et	Me	$CH_2OCONHEt$	$CH_2OCONHEt$	0.14
6	Bn	Me	$CH_2OCONHEt$	$CH_2OCONHEt$	0.14
7	Me	Me	CH_2OCONH*i*-Pr	CH_2OCONH*i*-Pr	0.03
8	Et	Me	CH_2OCONH*i*-Pr	CH_2OCONH*i*-Pr	0.14
9	Bn	Me	CH_2OCONH*i*-Pr	CH_2OCONH*i*-Pr	0.10
10	Me	Et	CH_2OH	CH_2OH	0.20
11	Me	C_6H_6	CH_2OH	CH_2OH	1.17
12	Me	4'-F-C_6H_4	CH_2OH	CH_2OH	1.46
13	Me	4'-Cl-C_6H_4	CH_2OH	CH_2OH	4.58
14	Me	3',4'-di-F-C_6H_3	CH_2OH	CH_2OH	7.94
15	Me	3'-Cl-4'-F-C_6H_3	CH_2OH	CH_2OH	14.37
16	Me	4'-MeO-C_6H_4	CH_2OH	CH_2OH	1.30
17	Me	3',4'-di-MeO-C_6H_3	CH_2OH	CH_2OH	0.96
18	Me	3',4',5'-tri-MeO-C_6H_2	CH_2OH	CH_2OH	4.45
19	Me	Et	$CH_2OCONHEt$	$CH_2OCONHEt$	0.16
20	Me	C_6H_6	$CH_2OCONHEt$	$CH_2OCONHEt$	0.23
21	Me	4'-F-C_6H_4	$CH_2OCONHEt$	$CH_2OCONHEt$	0.39
22	Me	4'-Cl-C_6H_4	$CH_2OCONHEt$	$CH_2OCONHEt$	0.35
23	Me	3',4'-di-F-C_6H_3	$CH_2OCONHEt$	$CH_2OCONHEt$	0.13
24	Me	3'-Cl-4'-F-C_6H_3	$CH_2OCONHEt$	$CH_2OCONHEt$	1.80
25	Me	4'-MeO-C_6H_4	$CH_2OCONHEt$	$CH_2OCONHEt$	0.10
26	Me	3',4'-di-MeO-C_6H_3	$CH_2OCONHEt$	$CH_2OCONHEt$	0.30
27	Me	3',4',5'-tri-MeO-C_6H_2	$CH_2OCONHEt$	$CH_2OCONHEt$	0.62
28	Me	Et	CH_2OCONH*i*-Pr	CH_2OCONH*i*-Pr	0.16
29	Me	C_6H_6	CH_2OCONH*i*-Pr	CH_2OCONH*i*-Pr	0.13
30	Me	4'-F-C_6H_4	CH_2OCONH*i*-Pr	CH_2OCONH*i*-Pr	0.11
31	Me	4'-Cl-C_6H_4	CH_2OCONH*i*-Pr	CH_2OCONH*i*-Pr	0.44
32	Me	3',4'-di-F-C_6H_3	CH_2OCONH*i*-Pr	CH_2OCONH*i*-Pr	0.44
33	Me	3'-Cl-4'-F-C_6H_3	CH_2OCONH*i*-Pr	CH_2OCONH*i*-Pr	1.91
34	Me	4'-MeO-C_6H_4	CH_2OCONH*i*-Pr	CH_2OCONH*i*-Pr	0.12
35	Me	3',4'-di-MeO-C_6H_3	CH_2OCONH*i*-Pr	CH_2OCONH*i*-Pr	0.30
36	Me	3',4',5'-tri-MeO-C_6H_2	CH_2OCONH*i*-Pr	CH_2OCONH*i*-Pr	0.95

Table 2: Experimental and Predicted pIC_{50} values of the test set

Molecule ID	Experimental pIC_{50}	Predicted pIC_{50} (CoMFA)	Predicted pIC_{50} (CoMSIA)	Predicted pIC_{50} (HQSAR)
1	9.869	9.6	9.57	9.621
3	9.108	9.38	9.29	9.211
5	9.509	9.29	9.69	9.654
22	9.184	9.41	9.4	9.079
29	9.609	9.39	9.89	9.578
31	9.107	9.38	9.31	9.297
33	8.483	8.87	8.83	8.201
34	9.667	9.87	9.76	9.552

Table 3: Experimental and Predicted pIC_{50} values of the training set

Molecule ID	Experimental pIC_{50}	Predicted pIC_{50} (CoMFA)	Predicted pIC_{50} (CoMSIA)	Predicted pIC_{50} (HQSAR)
2	9.491	9.3629	0.1281	9.184
4	10.039	10.2139	-0.1749	10.642
6	9.565	9.5281	0.0369	9.716
7	10.191	10.0181	0.1729	10.009
8	9.535	9.6547	-0.1197	9.950
9	9.734	9.8558	-0.1218	9.661
10	9.19	9.2201	-0.0301	8.831
11	8.486	8.3429	0.1431	8.626
12	8.411	8.1123	0.2987	8.416
13	7.933	8.1497	-0.2167	7.889
14	7.696	7.9928	-0.2968	8.101
15	7.456	7.6373	-0.1813	7.589
16	8.475	8.3955	0.0795	8.686
17	8.639	8.7283	-0.0893	8.426
18	8.003	7.8285	0.1745	7.992
19	9.451	9.3553	0.0957	9.629
20	9.337	9.2743	0.0627	9.563
21	9.123	9.0656	0.0574	9.353
23	9.615	9.4372	0.1778	9.038
24	8.487	8.6024	-0.1154	8.526
25	9.724	9.7534	-0.0294	9.623
26	9.271	9.1752	0.0958	9.363
27	8.978	8.9781	-0.0001	8.929
28	9.477	9.4761	0.0009	9.574
30	9.696	9.8921	-0.1961	9.299
32	9.108	9.1519	-0.0439	8.984
35	9.292	9.1752	0.1168	9.308
36	8.813	8.8383	-0.0253	8.875

Table 4: Statistical Data

PLS Statistics	CoMFA	CoMSIA	HQSAR
N	36	36	36
q^2	0.755	0.728	0.881
r^2	0.959	0.908	0.900
r^2_{pred}	0.713	0.768	-
r^2_{bs}	0.977	0.945	-
$r^2_{y\text{-}scrambling}$	0.1	0.15	-
F	81.487	34.692	-
SE	0.163	0.243	-
PLS Components	6	6	-
Field Contribution			-
			-
Steric	0.913	0.549	-
Electrostatic	0.087	0.356	-
H-bond acceptor	-	0.095	-
$r^2_{ensemble}$	-	-	0.894
Best length	-	-	97
Standard error (r^2)	-	-	0.254
Standard error (q^2)	-	-	0.413
Standard error ($r^2_{ensemble}$)	-	-	0.431

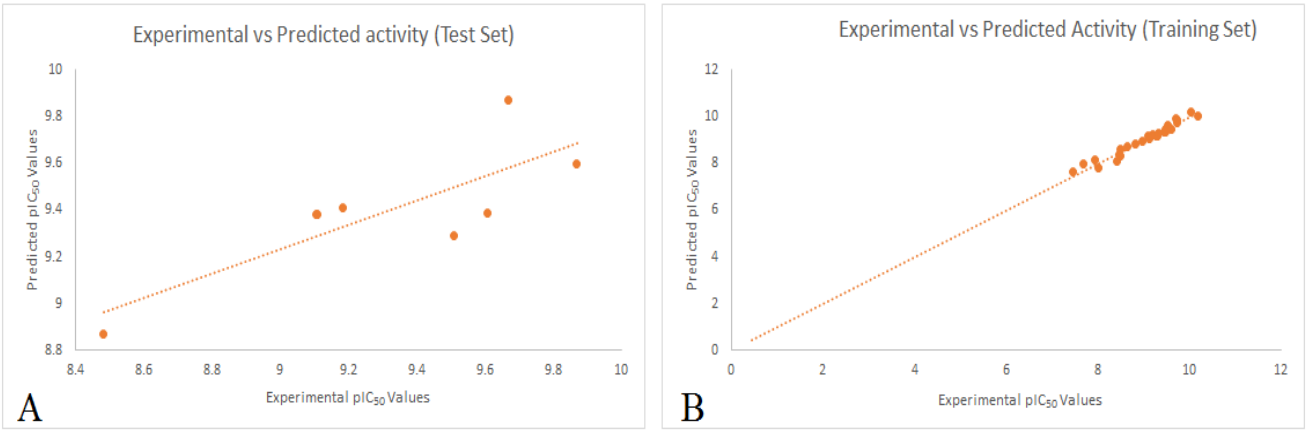

Figure 2: Experimental CoMFA Model

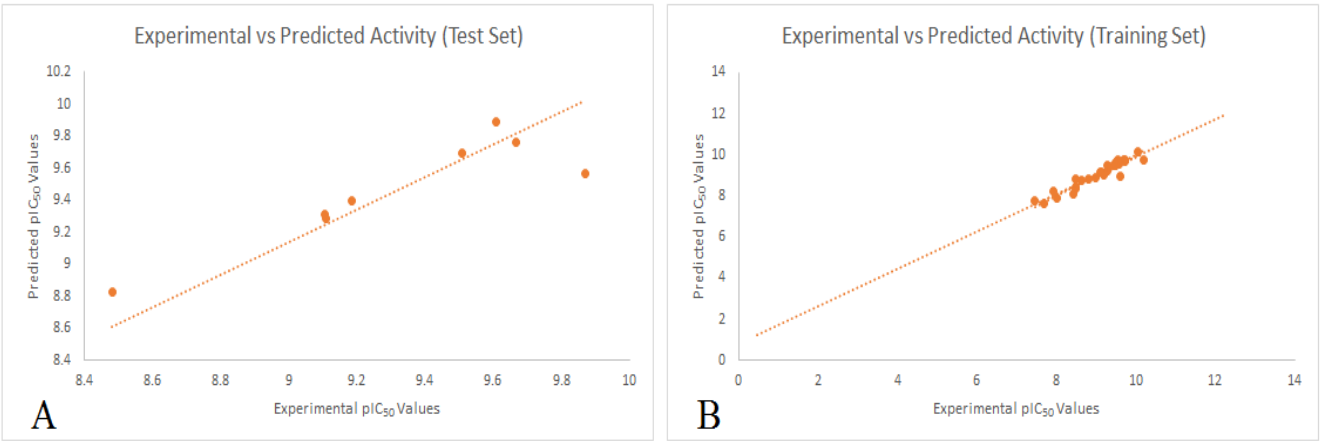

Figure 3: Experimental CoMSIA Model

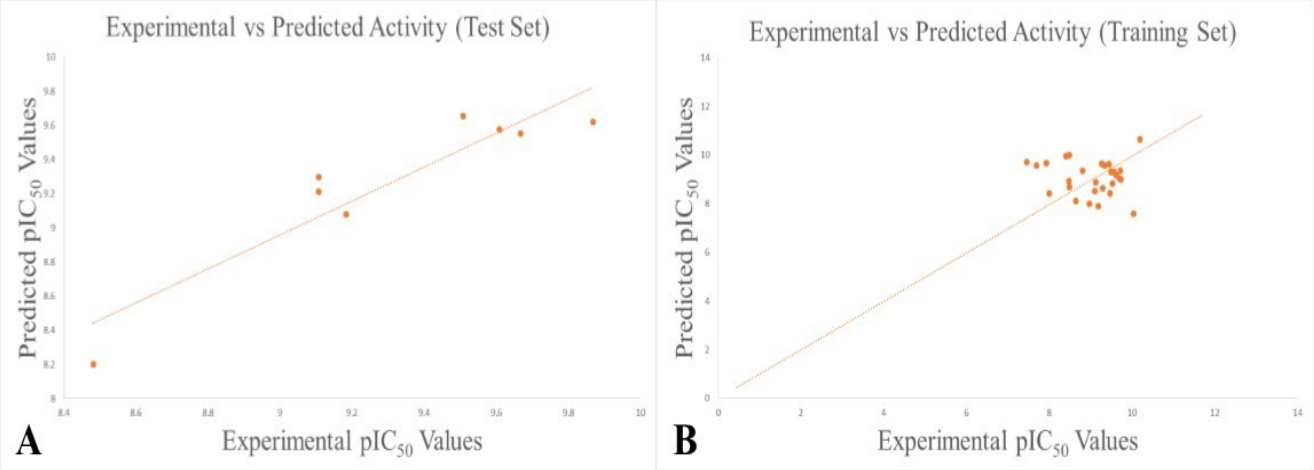

Figure 4: Experimental HQSAR Model

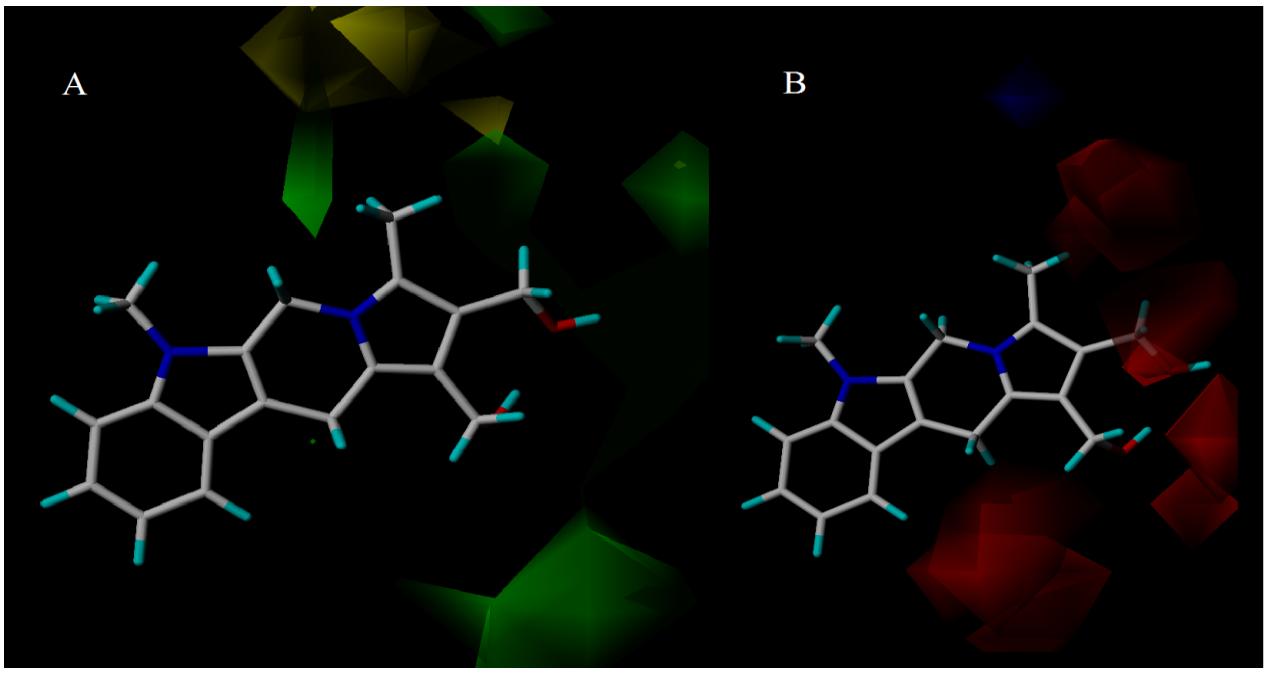

Figure 5: CoMFA Steric Contour Map (A) and CoMFA Electrostatic Contour Map (B)

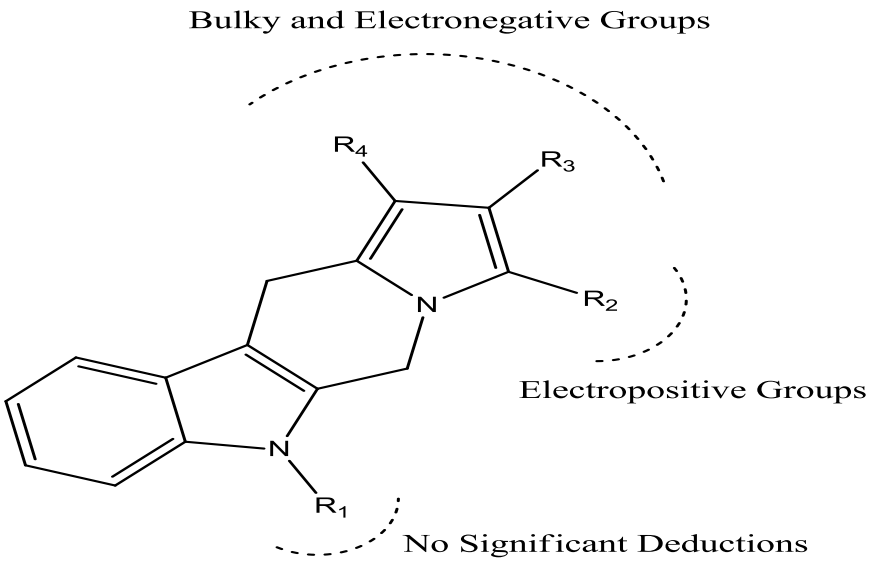

Figure 6: Graphical QSAR (CoMFA, CoMSIA and HQSAR) interpretation

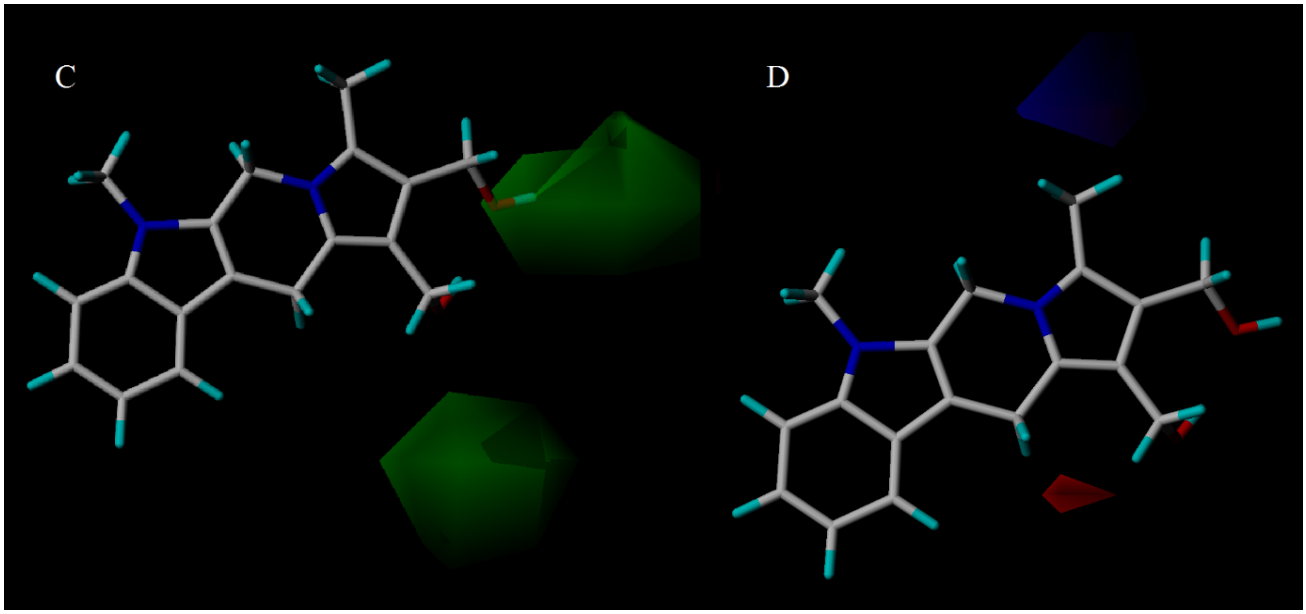

Figure 7: CoMSIA Steric Contour Map (C) and CoMSIA Electrostatic Contour Map (D)

REFERENCES

1. Wang, JC (1995), "DNA topoisomerases", ***Annu Rev Biochem***, Vol. 65, 635-692.
2. Kellner, U *et al.* (2002), "Culprit and victim -- DNA topoisomerase II", ***Lancet Oncol***, Vol. 3(4), 235-243.
3. Corbett, AH and Osheroff, N (1993), "When good enzymes go bad: conversion of topoisomerase II to a cellular toxin by antineoplastic drugs", ***Chem Res Toxicol***, 1993. Vol. 6(5), 585-597.
4. Dancey, J and Eisenhauer, EA (1996), "Current perspectives on camptothecins in cancer treatment", ***Br J Cancer***, Vol. 74(3), 327-338.
5. Pommier, Y (2009), "DNA topoisomerase I inhibitors: chemistry, biology, and interfacial inhibition", ***Chem Rev***, Vol. 109(7), 2894-2902.
6. Hande, KR (2008), "Topoisomerase II inhibitors", ***Update on Cancer Therapeutics***, Vol. 3(1), 13-26.
7. Utsugi, T *et al.* (1997), "Antitumor activity of a novel quinoline derivative, TAS-103, with inhibitory effects on topoisomerases I and II", ***Jpn J Cancer Res***, Vol. 88(10), 992-1002.
8. Denny, WA and Baguley, BC (2003), "Dual topoisomerase I/II inhibitors in cancer therapy", ***Curr Top Med Chem***, Vol. 3(3), 339-353.
9. Salerno, S *et al.* (2010), "Recent advances in the development of dual topoisomerase I and II inhibitors as anticancer drugs", ***Curr Med Chem***, Vol. 17(35), 4270-4290.
10. Chaniyara, R *et al.* (2013), "Novel antitumor indolizino[6,7-b]indoles with multiple modes of action: DNA cross-linking and topoisomerase I and II inhibition", ***J Med Chem***, Vol. 56(4), 1544-1563.
11. Mishra, H; Parrill, AL and Williamson, JS (2002), "Three-dimensional quantitative structure-activity relationship and comparative molecular field analysis of dipeptide hydroxamic acid Helicobacter pylori urease inhibitors", ***Antimicrob Agents Chemother***, Vol. 46(8), 2613-2618.
12. Klebe, GU Abraham and Mietzner, T (1994), "Molecular similarity indices in a comparative analysis (CoMSIA) of drug molecules to correlate and predict their biological activity", *J Med Chem*, Vol. 37(24), 4130-4146.
13. Bohm, M; Strzebecher, J and Klebe, G (1999), "Three-dimensional quantitative structure-activity relationship analyses using comparative molecular field analysis

and comparative molecular similarity indices analysis to elucidate selectivity differences of inhibitors binding to trypsin, thrombin, and factor Xa", ***J Med Chem***, Vol. 42(3), 458-477.

14. Wold, SE; Johansson and , M (1993), "PLS: partial least squares projections to latent structures. 3D QSAR in drug design: theory, methods and applications", ***Leiden: ESCOM Science***.
15. Stone, M (1974), "Cross-Validatory Choice and Assessment of Statistical Predictions", ***Journal of the Royal Statistical Society, Series B (Methodological)***, 111-147.
16. Cramer, RD *et al.*, "Crossvalidation, Bootstrapping, and Partial Least Squares Compared with Multiple Regression in Conventional QSAR Studies", ***Quantitative Structure-Activity Relationships***", Vol. 7(1), 18-25.
17. Bush, BL and Nachbar, Jr RB (1993), "Sample-distance partial least squares: PLS optimized for many variables, with application to CoMFA", ***J Comput Aided Mol Des***, 7(5), 587-619.

Correspondence Author:
Sachin Wakadkar
Department of Pharmaceutical Chemistry, Sinhgad College of Pharmacy, STES Campus, Off Sinhagad Road, Pune-411 041, India

Cite This Article: Anuj, Kale; Sachin, Wakadkar; Madhuri, Nagras and Vijay, Khedkar (2014), "2D and 3D QSAR studies of Indolizino[6,7-b] indole derivatives as topoisomerase I and II dual inhibitors", ***Pharmacophore***, Vol. 5 (6), 857-866.